JOURNAL OF BACTERIOLOGY, Feb. 1978, p. 995-1007
0021-9193/78/0133-0995$02.00/0

Vol. 133, No. 2
Printed in U.S.A.

Production of Giant Cells of *Escherichia coli*

W. S. LONG,[1]* C. L. SLAYMAN,[1] AND K. B. LOW[2]

Department of Physiology[1] and Department of Therapeutic Radiology,[2] Yale University School of Medicine, New Haven, Connecticut 06590

Received for publication 20 October 1977

Giant cells, with volumes up to 500-fold those of normal cells, have been produced by both genetic and pharmacological means in *Escherichia coli* K-12. In the genetic approach, an *envB* or *mon* mutation (conferring rounded or irregular morphology) was combined with a *lon* mutation (block of septation after irradiation). UV irradiation and subsequent incubation for 2 to 5 h in a rich medium supplemented with 1% sodium chloride led to production of polymorphic giant cells. In the pharmacological approach, incubation of several different strains of *E. coli* K-12 with the drug 6-amidinopenicillanic acid (FL1060) in the same rich medium gave rise to a homogeneous population of smoothly rounded giant cells.

In 1968, H. I. Adler and his co-workers reported the construction of the first strain of *Escherichia coli* to produce giant cells (1). This strain, P678-A4, was a recombinant of a cross between a *lon*-bearing strain (3.300-M6) and a strain (P678-7) with cells of irregular geometry and no constant plane of division. (The genetic locus for abnormal morphology, designated *mon* in P678-7, was not identified.) Since *lon*, under a variety of conditions including mild doses of irradiation, inhibits division but allows growth, Adler et al. reasoned that growth of *mon lon* recombinants "in all directions" would produce giant cells after irradiation. X-irradiation of P678-A4 did indeed produce giant cells estimated to have 500 to 1,000 times the volume of normal *E. coli* when grown on agar slips. The largest volumes for irradiated cells of P678-A4 grown in suspension were later estimated at approximately 900 μm^3 (2).

Our interest in giant cells of *E. coli* was prompted by development of the "chemiosmotic" hypothesis for oxidative phosphorylation, which requires that large membrane potentials exist to couple respiratory processes to formation of ATP (17). It seemed likely that strain P678-A4 would make possible the insertion of microelectrodes and direct measurement of membrane potentials, and thereby a direct test of the chemiosmotic hypothesis. However, our efforts to repeat the generation of giant cells from P778-A4 were unsuccessful, perhaps because of an unknown alteration in the strain (H. I. Adler, personal communication). One other strain that produces very large cells during growth at high temperature (temperature-sensitive lesion) has been reported (10), but no genetic analysis of the strain has been published, which greatly limits its usefulness at the present time.

In this paper, we describe two approaches to giant-cell production. In the first, the rationale of Adler was followed, and two mutations were combined (i) to inhibit septation and (ii) to convert cells from the usual rod to rounded or amorphous shapes. By adding these two morphological variations, we have constructed strains that produce giant cells similar to those originally described (1). In the second approach, the drug 6-aminidinopenicillanic acid (FL1060) (8) has been used to inhibit cell elongation and septation. Under the proper conditions, cells growing in the presence of this drug assume a uniform spherical shape and grow in volume to a size of 100 to 500 μm^3 (in some cases, to 1,000 μm^3). Cells in this size range persist in the culture for several hours.

MATERIALS AND METHODS

Strains of *E. coli* K-12. *E. coli* strains used are listed in Table 1, with all their known mutant alleles.

Media. Cells were grown in four liquid media: (i) Luria broth (LB), modified to contain 1% tryptone broth, 0.5% yeast extract, and 0.05% NaCl, at pH 7; (ii) LB containing 1% NaCl (NaLB); (iii) 56 minimal medium (12) (usually diluted twofold and, therefore, designated 56/2); and (iv) modified giant-cell broth (NaGCB), containing 1% NaCl, 4.5% nutrient broth, 0.4% yeast extract, 7.8 mM KH_2PO_4, and 12.2 mM K_2HPO_4, at pH 6.8 to 7.0 (1).

Plating media contained 1.5% dissolved agar. Amino acids and nucleosides, when required, were added to 56/2 minimal medium at a final concentration of 50 μg/ml; vitamins were added at 0.1 μg/ml. The supplement for $AroE^-$ strains contained phenylalanine, tyrosine, tryptophan, and shikimic acid at 10^{-6} M. Difco MacConkey agar plates contained sugars at a final

TABLE 1. *E. coli K-12 strains used*[a]

Strain	Genotype	Source or derivation
W3110	F⁻ λ⁻	B. J. Bachmann, CGSC
P678-7	F⁻ *thi-1 thr-1 leu-6 lacY1 mtl-2 xyl-7 malA1 ara-13 gal-6 tonA2* λʳ λ⁻? *strA135 supE44? mon-1*	H. I. Adler (1)
P678-A4	As for P678-7 but *lon-10* (*capR6*)	H. I. Adler (1), 3.300-M6 × P678-7
D23	F⁻ *his-51 trp-30² pro-23 lac-28 str-173 ampA1 sloB1 envB1 tsx-81*	S. Normark (18)
3.300-M6	Hfr Cavalli *thi-1 rel-1 lacI22* λ⁻ *lon-10* (*capR6*)	A. Markovitz (1)
AB2834	F⁻ *aroE53 mal-352 tsx-352* λʳ λ⁻ *supE42?*	B. J. Bachmann, CGSC
G11a1	Hfr Cavalli *metB1 ilv-299 rel-1 ampA1*	B. J. Bachmann, CGSC (18)
KL266	F⁻ *thi-1 metE70 leu-6 proC32 malA38 hisF860 thyA54 cysC43 lacZ36 ara-14 mtl-1 xyl-5 str-109 spc-15* λ⁻ and uncharacterized mutation near *his* conferring Mal⁺ phenotype	K. B. Low (11)
KL295	Hfr Cavalli *pro-48* λ⁻	K. B. Low, unpublished
KL297	F8(*gal*⁺)/*thi-1 metE70 leu-6 proC32 malA38 hisF860 cysC43 lacZ36 ara-14 mtl-1 xyl-5 str-109 spc-15* λ⁻ and uncharacterized mutation near *his* giving Mal⁺	K. B. Low, unpublished
JM888	Hfr KL16 *tif-1 malA26*	J. George
BU8049	F⁻ Δ(*pro-lac*) *rpsL degTa* (*lon*)	B. Apte
LL81	F⁻ *his-51 str-173 ampA1 envB1 sloB1 lon-10* (*capR6*)	3.300-Mg × D23 → Pro⁺ or Lac⁺ [Strʳ][b]
LL57	F⁻ *aroE353 mal-352 ampA1 metB1*	G11a1 × AB 2834 → Ampʳ [Ilv⁺]
LL58	As for LL57 but *thy*⁻	Spontaneous Thy⁻ from LL57
LL59	As for LL57 but *metB*⁺	G11a1 × AB 2834 → Ampʳ [Ilv⁺]
LL6	F8(*gal*⁺)/*thi-1 metE70 leu-6 proC32 aroE353 cysC43 mal-352* and/or *malA38 lacZ36 mtl-1 xyl-5 ampA1*	KL297 × LL58 → Ampʳ Thy⁺ [His⁺]
LL7	As for LL6 but *lon-10* (*capR6*) *pro*⁺	P1 · LL81 × LL6 → Pro⁺
LL8 & 9	As for LL7 but *envB1 rpsL*⁺ *aro*⁺	P1 · D23 × LL7 → Aro⁺
LL10	As for LL8 but *pro-48 lon*⁺	KL295 × LL8 → Lac⁺ [Ampʳ]
LL11	As for LL6 but *rpsL135 mon-1 aro*⁺	P1 · P678-A4 × LL6 → Aro⁺
LL12	As for LL11 but *degTa pro*⁺	P1 · BU8049 × LL11 → Pro⁺
LL13	As for LL11 but *tif-1 cysC*⁺	JM888 × LL11 → Cys⁺ [Strʳ]
LL14	As for LL12 but *tif-1 cysC*⁺	JM888 × LL12 → Cys⁺ [Strʳ]
LL2683	As for D23 but *rpsE*	Spontaneous Spcʳ from D23

[a] The allele numbers are registered with the Coli Genetic Stock Center (CGSC).
[b] A Trp⁺ revertant of D23 was used to produce LL81.

concentration of 1%. Mitomycin C, streptomycin sulfate, and spectinomycin were added to LB at concentrations of 0.5, 100, and 50 μg/ml, respectively.

Bacterial matings and transductions. Bacterial matings and transductions performed have been described previously (12, 13). The presence of *sloB1*, an allele responsible for slow growth of D23 (21) (see Table 1), was tested by streaking purified colonies on supplemented minimal medium. SloB⁻ strains required 36 to 48 h for full growth at 37°C; *sloB*⁺ strains required 18 to 24 h. Comparison of doubling times for log-phase suspensions at 37°C differentiated the strains' designations in accordance with the plating test and the test of Westling-Häggström and Normark (23).

The presence of *tif-1* was determined on supplemented minimal plates by differential survival of strains on media containing adenine (100 μg/ml) or guanosine and cytidine (100 μg/ml) at 42°C. Adenine promotes thermoinducible filamention, whereas the two nucleosides protect against it (9). For growth in suspension, the same concentrations and temperatures were used, and sucrose or mannitol was added for osmotic protection.

Ampicillin tests. Sensitivity to ampicillin (Principen; E. R. Squibb & Sons, Inc., N.Y.) was tested by survival of test colonies on plates containing 0, 10, and 25 μg of ampicillin per ml of NaLB using double-velvet replication, as follows. For characterization of recombinant and transductant colonies, the master

grids on supplemented minimal selection media were replicated on NaLB plates. After the appearance of visible new patches, the NaLB master grids were stamped on a sterile velvet, and the first plate (LB) copied was set aside until all other test plates had been replicated. The LB copy of the master plate was then stamped on a fresh sterile velvet, and the ampicillin test plates were copied in the order 0, 10, 25 μg of ampicillin per ml of NaLB. The plates were incubated at 40°C for 8 to 24 h (depending on the strain) before reading. Purification and recharacterization clarified ambiguous results from master grids.

Giant-cell induction with UV irradiation. Giant-cell-producing strains were grown at 37°C to log phase (optical density value at 650 nm ≈ 0.2) in NaGCB after 1:50 to 1:20 dilution of overnight suspensions into NaGCB. Thin (2 to 3 mm) NaGCB agar plates were washed with 0.8 ml of the log-phase suspensions, drained, and dried at 37°C. The cells were irradiated at 150 ergs/mm^2 with a Sylvania G15T8 germicidal lamp and incubated for 2 to 5 h before inspection. The fluence rate was 10 ergs/mm^2 per s and was measured with a Latarjet dosimeter.

Giant-cell induction with FL1060. FL1060 was generously donated by Leo Pharmaceutical Products of Ballerup, Denmark. The drug was added to log-phase suspensions of about 10^7 cells per ml of NaLB or NaGCB for final concentrations of 0.1, 0.3, or 1 μg/ml. At 1 to 3 h after addition of the drug, a single drop of suspension was placed on a thin layer of agar, dried, and photographed. In some cases, the suspension was plated on a thin-layer agar plate containing the drug at the same concentration as the liquid medium. Half the plates received UV irradiation before incubation, and the others were incubated at 37°C without irradiation.

Photomicroscopy. Cells in suspension were viewed directly on glass slides under cover slips; irradiated cells and their supporting agar were cut from the plate and mounted. In some cases, a drop of log-phase cells was dried on an agar slip and then mounted for viewing.

For phase photomicroscopy of living cells, a Zeiss model WL microscope with camera attachment was employed. Kodak Tri-X film was used, and, at magnifications of ×400 or less, exposure times under 2 s were sufficient. Surface areas for the time-lapse studies were measured with a compensating polar planimeter (Gelman Instruments) calibrated with a micrometer photographed at the appropriate magnification.

For stained preparations, suspensions of log-phase cells or of irradiated cells washed from the agar plates with NaGCB were smeared on glass slides with cover slips and then heat fixed. The slides were flooded with 0.08% gentian violet, gently heated, and washed. Although washing removed many cells, the edges of each smear offered a good collection for photomicrography. The stained specimens were examined and photographed with a standard Zeiss Photomicroscope (POL), using ×50 and ×80 Neofluor objectives, a yellow filter (Zeiss GG11), and Kodak Pan-X film.

RESULTS

Derivation and initial characterization of LL81, a new giant-cell-producing strain. In searching for a combination of alleles that would produce giant cells, we chose as the morphological mutant strain D23, originally described by Normark (18). Like P678-7 and P678-A4, D23 in log-phase suspension produces heteromorphic populations of irregular cells, generally two to five times the normal cellular volume of, for example, W3110. The aberrant morphology is associated with the *envB1* locus situated near the *rpsL* region on the *E. coli* K-12 genetic map (4). The presence of *envB1* in conjunction with *ampA* confers intermediate sensitivity to ampicillin (sensitive at 25 μg of ampicillin per ml of agar) when compared to AmpA$^+$ EnvB$^+$ strains (sensitive at 10 μg/ml) and AmpA$^-$ EnvB$^+$ (resistant at 25 μg/ml). Both ampicillin sensitivity and irregular morphology were used by Normark to describe *envB1* in D23 (18). Ampicillin sensitivity, as well as the mapping data, made this mutant more attractive as a morphological mutant than P678-7. Like Adler, we used 3.300-M6 as a source of *lon*. From a cross of 3.300-M6 × D23, seven of eight randomly purified Pro$^+$ Str^r recombinants and four of seven Lac$^+$ Str$^+$ recombinants produced giant cells after induction with UV irradiation. One, LL81, was selected for further study.

Giant cells grown on thin NaGCB agar plates after UV irradiation were shaped like pancakes. With an estimated thickness of 1.5 to 2 μm, the largest cells ranged in volume from 200 to 500 μm^3 at 5 h after irradiation. Figure 1 shows a stained preparation of LL81. Although heat fixation has produced some distortion, as can be appreciated from the phase micrograph of Fig. 2, the heteromorphic character of the population, the size of the cells, and even some cytoplasmic features, such as vacuolation, can be seen. The induced (irradiated) cultures showed marked morphological heterogeneity, including not only giant cells but bizarre forms (length/width = 3 to 10) and irregularly shaped filaments (length/width > 10). In a typical experiment, LL81 produced 12% giant cells, 76% bizarre forms, 8% filaments, and 4% smaller forms among 171 cells examined 5 h after irradiation. At 8 h, many cells appeared disrupted, and the surviving population contained 41% giant cells, 26% bizarre forms, 17% filaments, and 16% smaller forms (N = 58). Many of the disrupted cells appeared to have reached the size of giant cells before disintegration.

Irradiation of M6 under the same conditions produced only long filaments of a constant diameter approximately equal to that of the log-phase rods. Irradiation of D23 gave rise to a population of bizarre forms, 10 to 20% the volume of the LL81 giant cells.

The *aroE* region and abnormal morphology. We undertook a study of the *rpsL-aroE-envB* region of the chromosomes in D23 and

FIG. 1. *Giant cells of strain LL81 5 h after irradiation. Cells were washed from thin agar plates, heat fixed, and stained on slide with gentian violet.*

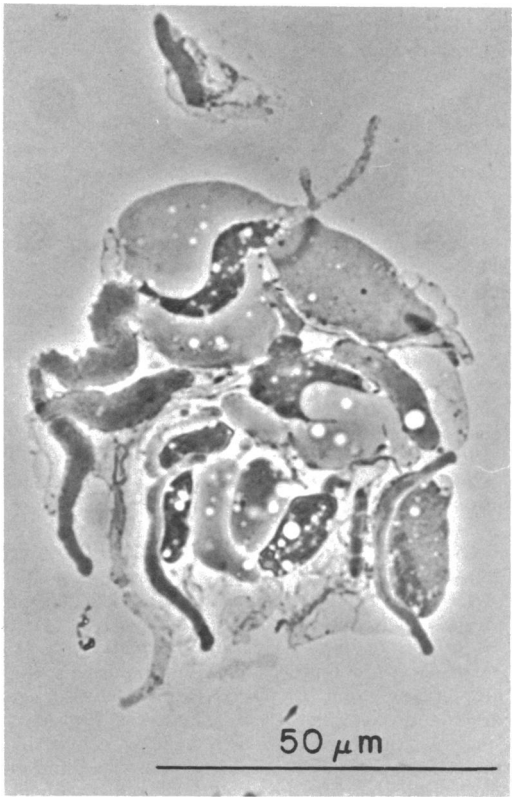

FIG. 2. *Phase microphotograph of a cell cluster from strain LL81 in situ on NaGCB agar, 5 h after irradiation.*

LL81 to clarify the involvement of genes in that region in the irregular morphology necessary to induction of giant cells. LL59 was transduced with P1 phage grown on D23 or LL81, with selection for Aro$^+$. Tables 2 and 5 present the cotransduction frequencies and the classification of the purified transductants into eight classes on the basis of the three phenotypic markers, Slo, Str, and Morph.

The data indicate that there exist no obvious dissimilarities in the *rpsL-aroE-envB* regions of the chromosomes of D23 and LL81. The lack of quantitative identity between the two strains we attribute to the small number of transductants tested.

The cotransduction frequencies show close linkage between *sloB1* and *rpsL*, and the order assigned to them in Table 2 is based upon the absence of transductants in classes III and IV. Assignment of *sloB1* to a position between *rpsL* and *aroE* would have required two pairs of crossovers to account for classes V and VI. This placement of *sloB1* substantiates the findings of Westling-Häggström and Normark (23) published during the course of these experiments; the order *rpsL-aroE-envB1* has been previously established (18).

In Table 2 we have expressed the cotransduction frequencies and class distribution on the basis of phenotype. The relationships of Slo to *sloB1* and Str to *rpsL* appear straightforward; but the two phenotypic criteria for *envB1*, i.e., ampicillin sensitivity and morphology, are problematic. Both criteria are valid in classes V through VIII, i.e., Aro$^+$ Amp^s transductants in classes VI and VIII are morphologically different from the rods of classes V and VII and the

TABLE 2. *Aro⁺ transductants: P1 · D23 (sloB rpsL aroE⁺ envB) × LL59 (sloB⁺ rpsL⁺ aroE envB⁺) and P1 · LL81 (sloB rpsL aroE⁺ envB) × LL59*

Class	Phenotype			P1 · D23 × LL59		P1 · LL81 × LL59		Amp_{25}[b]	
	Slo	Str	Morph[a]	Frequency	*N*	Frequency	*N*	Expected	Observed
I	−	R	+	0.47[c]	49	0.370	37	R	S
II	−	R	−		0		0	S	
III	−	S	+		0		0	R	
IV	−	S	−		0		0	S	
V	+	R	+	0.04	4	0.010	1	R	R
VI	+	R	−	0.01	1		0	S	S
VII	+	S	+	0.39	41	0.570	57	R	R
VIII	+	S	−	0.09	10	0.050	5	S	S

[a] Morph: +, normal rods; −, abnormal shapes.
[b] AMP_{25}, 25 μg of ampicillin per ml. R, Resistant; S, sensitive.
[c] Frequency for class I based on Slo⁻ Str^r Amp^s_25 (Amp^s_{25}, sensitivity to 25 μg of ampicillin per ml) phenotype; see text for explanation.

recipient parent LL59. However, in the Slo⁻ Str^r Aro⁺ classes I and II, the phenotypic criteria are dissociated. Slo⁻ Str^r Aro⁺ Amp^s transductants are rod shaped rather than irregular. If one adopts the morphological criterion for *envB1*, these transductants belong to class I and our data (5 to 10%) approximate the *aroE⁺-envB1* cotransduction frequency published by the Swedish workers (6 to 9%). Because we tested the morphology of one-half the Aro⁺ transductants (48 for P1 · LL81 × LL59 and 49 for P1 · D23 × LL59), we cannot divide the Slo⁻ Str^r Aro⁺ classes with certainty. All 34 transductants of this phenotype checked, however, were rods.

The morphological phenotype seems a more reliable index of *envB1* transduction than Amp^s. When selection for Str^r instead of Aro⁺ was applied in the transductions, the Str^r Amp^s transductants were two to three times more numerous than the Str^r Aro⁺ transductants. It is more reasonable to assume that Amp^s is a poor criterion for *envB1* than to assume an excessively high frequency of double crossovers in the transductions. Similarly, with regard to the transduction reported in Table 2, it is unlikely that two markers separated by 2 min on the map (*rpsL* and *envB1*) should be cotransduced at such a high frequency when *rpsL* and *aroE⁺*, separated by only 0.5 min, are not cotransduced.

The dissociation of ampicillin sensitivity and abnormal morphology in the transduction described indicates that another locus in the region *sloB1-aroE* is involved in determining the Amp^s phenotype. The *sloB1* locus does not by itself account for the dissociation, since both abnormal morphology and ampicillin sensitivity characterize D23 (*sloB1 rpsL envB1*, no dissociation) and since the dissociation of phenotypic markers is also found in Aro⁺ transductants derived from P1 · P678-A4 × LL59, where P678-A4 is *SloB⁺* (see below). The data do not exclude other sites in the region between *sloB1* and *aroE;* however, Str^r characterizes all transductants showing dissociation (see Discussion).

A correction of the dissociation of phenotypes for *envB1* was found when LL59 was transduced with P1 grown on a spontaneous spectinomycin-resistant (100 μg/ml), fast-growing revertant of D23. Table 3 presents the results of the transduction (see also Table 5).

The table shows that the major class of Str^r transductants were Amp^r and rod shaped, in contrast to the Str^r Amp^s rod-shaped transductants in Table 2. In addition, the single Str^r Spc^s Amp^s transductant was also a rod, whereas the two Str^r Spc^r Amp^s transductants were irregular or rounded rods. Similarly, in class VIII the Spc^r transductants were more abnormal in morphology than the Spc^s subclass, and neither class showed the rod forms of the recipient parent. By contrast, the assignment of Spc phenotype in Amp^r transductants had no effect on the uniform rod morphology. Although the number of transductants considered is small, we can make the tentative conclusion that a locus in the *rpsE* region of the chromosome is involved in modifying the ampicillin sensitivity of the *envB* locus.

The classifications of Aro⁺ transductants and cotransduction frequencies are similar to the data published for the linkage of *envB* to *aroE* and *rpsL* (23) and for linkage of *rpsE* to *aroE* and *rpsL* (3).

Location of *mon* on the genetic map. Because the mating 3.300-M6 × D23 produced giant-cell strains as had Adler's cross, 3.300-M6 × P678-7, and because the aberrant morphologies of P678-7 and D23 were similar, we tested

TABLE 3. *Aro⁺ transductants: P1 · LL2683 (rpsL rpsE aroE⁺ envB) × LL59 (rpsL⁺ rpsE⁺ aroE envB⁺)*

Class	Phenotype[a]				Frequency	*N*
	Str	Spc	Amp_{25}	Morph		
V R	R	R	R	Rods	0.55	133
V S	R	S	R	Rods	0.004	1
VI R	R	R	S	Rounded rods, irregular	0.008	2
VI S	R	S	S	Rods	0.004	1
VII R	S	R	R	Rods	0.18	45
VII S	S	S	R	Rods	0.21	50
VIII R	S	R	S	Rounded rods, irregular	0.02	5
VIII S	S	S	S	Irregular	0.02	6

[a] Amp_{25}, 25 μg of ampicillin per ml. R, Resistant; S, sensitive.

the possibility that *envB* and *mon* were closely linked on the genetic map. LL59 was transduced with P1 grown on P678-A4, and the Aro⁺ transductants were tested for Str and Amp phenotypes (P678-A4 is Slo⁺). Table 4 presents the analysis of 181 transductants (see also Table 5).

Ampicillin sensitivity was cotransduced with *aroE*⁺ at approximately the same frequency observed for *envB1* in D23. Furthermore, the Str^s Amp^s transductants showed the irregular morphology of the donor strain. These observations constitute strong evidence that the *mon-1* and *envB1* loci are closely linked genetically and physiologically.

The cotransduction frequencies indicate that *aroE* lies equidistant between *rpsL* and *mon-1* when *mon-1* is characterized phenotypically by Amp^s. The results for classes V and VI show the same improbable distribution of Amp^s found in classes (I + V) and (II + VI) for Aro⁺ transductants of Pl · D23 × LL59, i.e., that the transductant class requiring the crossovers closest to the selected marker is smaller than that requiring integration of the largest segment of the donor genome. Using abnormal morphology rather than Amp^s as the phenotypic marker for *mon-1*, we found that 2 class VI transductants, of 39 examined for morphology, showed the donor parental strain's irregular geometry. Readjustment of classification, therefore, gives a cotransduction frequency of 9% for *aroE*⁺–*mon-1*. The dissociation of ampicillin sensitivity and abnormal morphology is thus present in both *envB1*- and *mon-1*-bearing Aro⁺ Str^r transductants.

The dependence of giant-cell production on *lon, mon, envB,* and *tif.* LL6 was constructed as a strain bearing mutations in *ampA, aroE, proC,* and *cysC* to obtain by transduction derivative strains with *proC*⁺ *capR* or *degTa, aroE*⁺ *envB1* or *mon* and *cysC*⁺ *tif* in various combinations. We have used these strains to determine the effect of the five mutant alleles on giant-cell production after UV irradiation or thermoinduction.

TABLE 4. *Aro⁺ transductants: P1 · P678-A4 × LL59*

Class	Phenotype			Frequency	*N*
	Str	Amp	Morph		
V	R	R	Rods	0.07	12
VI	R	S	Rods; rounded rods (2 of 39 tested)	0.54	98
VII	S	R	Rods	0.31	56
VIII	S	S	Irregular, some very small	0.08	15

capR and *degTa* mutations are both allelic to *lon* (6, 14), yielding filaments after irradiation. *envB* and *mon* are closely related genetically and physiologically, as described above. The *tif*-bearing strains are thermoinducible for filamentation (9). *lon tif* strains produce longer filaments after thermoinduction than strains bearing only *tif* (7).

LL7 is a mitomycin-sensitive strain with rod-shaped cells, and LL8 and LL9 are *envB capR* strains from the transduction P1 · D23 × LL7. Only Amp^s derivatives of LL7 produced cells of irregular shape in log-phase suspension and produced a heteromorphic population including giant cells after irradiation. Amp^r transductants were rods and produced filaments after induction. Irradiation of LL10, a *lon*⁺ *envB1* strain derived from LL8, produced a heteromorphic collection of bizarres but no giant cells; this pattern mimics that found after irradiation of D23.

LL11 is an Amp^s strain derived by transducing LL6 with P1 grown on P678-A4. LL12 is a *mon-1 degTa* strain, sensitive to mitomycin C and ampicillin. Both strains showed the irregular morphology of P678-A4 in log-phase suspensions, and both produced giant cells among the typical heteromorphic population after induction with UV light. The Amp^r strain from these transductions produced rods, chains, and filaments in log-phase suspension and filaments after irradiation.

The addition of *tif* to LL11 and LL12 produced

TABLE 5. *Summary of cotransduction frequencies*

Phenotype	P1 · D23 × LL59	P1 · LL81 × LL59	P1 · P678-A4 × LL59	P1 · LL2683 × LL59
Aro$^+$-Str^r	0.51	0.38	0.61	0.56
Aro$^+$-Amp$^s{}_{25}$[a]	0.57	0.42	0.62	0.06
Aro$^+$-Morph$^-$	0.10	0.05	0.09[b]	0.05
Aro$^+$-Spc^r				0.76
(*N*)	(105)	(100)	(181)	(243)

[a] Amp$^s{}_{25}$, Sensitivity to 25 μg of ampicillin per ml.
[b] Aro$^+$ abnormal morphology calculated by transferring 98% (38 of 39) Str^r-Amp^s transductants into class I.

strains that could be induced to give rather small giant cells (20 to 50 times the cellular volumes of normal *E. coli*) after either UV irradiation or elevation of the incubation temperature from 37 to 42°C (Fig. 3).

In some cases, *tif* transductants of LL11 or LL12 produced rod-shaped cells and filaments in log suspension in either NaLB or the supplemented minimal medium; these strains produced filaments after irradiation. Because of morphological instability in strains producing giant cells, we were unable to determine whether such filament formation was the result of interaction between *tif* and the other mutant alleles or the results of some independent transition in the *lon, mon-1,* or *envB1* loci.

From this series of transductions, we conclude that giant cells can be induced in strains carrying an allele for irregular geometry and either *lon* or *tif* or both. Their interaction produces giant cells in a variety of genetic backgrounds.

Giant-cell production with FL1060. FL1060 at concentrations of 0.2 μg/ml has been reported to produce rounded cells in log-phase suspensions of *E. coli* (16). (The strain markers were not specified.) As described, the population was fairly uniform, with some asymmetric central constrictions noted; the largest cells were 2.5 to 3 μm long and 1.5 to 2 μm wide. Because D23 and P678-A4 and strains derived from them show similar but more exaggerated morphology, we tested the effects of prolonged exposure to FL1060 on several strains from Table 1.

Figure 4 shows the effect on BU8049 of UV irradiation (150 ergs/mm^2) with (A) and without (B) preincubation for 90 min in FL1060 (1 μg/ml). Without the drug, irradiation produced filaments about 100 μm long. After treatment with FL1060, irradiation produced a rather uniform population of giant cells ranging from 10 to 25 μm in diameter. All larger cells possessed at least one prominent vacuole. The morphological response noted in BU8049 does not depend upon *lon*; the wild-type strain W3110 gave a similar response to the same treatments.

Figure 5 illustrates the effect of FL1060 on LL9 (*lon envB1*) with and without irradiation. Figure 5A shows untreated log-phase cells; the

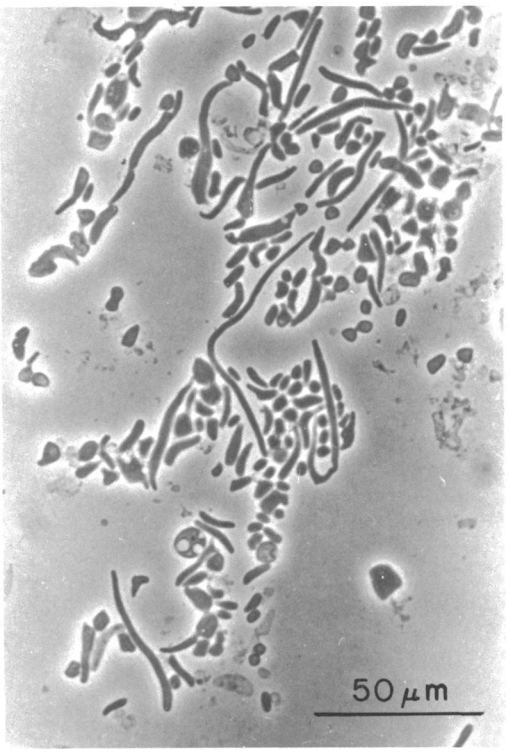

FIG. 3. *Phase photomicrograph of LL13 grown in 56/2 minimal medium + Casamino Acids + adenine + mannitol. A drop of suspension was dried on an agar slip at 37°C and photographed through a cover slip.*

population has the heteromorphy typical of *envB1*-bearing strains. The largest cells are about 10 μm long and 5 μm wide; most are considerably smaller. In Fig. 5B, the cells were exposed for 90 min to 0.3 μg of FL1060 per ml in suspension, then plated and incubated for 3 h at 35°C. The strain shows some thick rods and filaments, but a preponderance of rounded, vacuolated giant cells, ranging from 6 to 20 μm in diameter. Figure 5C presents cells treated as in B but receiving UV irradiation before the 3-h incubation. This culture has the same array of forms, but the giant cells are generally larger than those exposed only to the drug. Note that

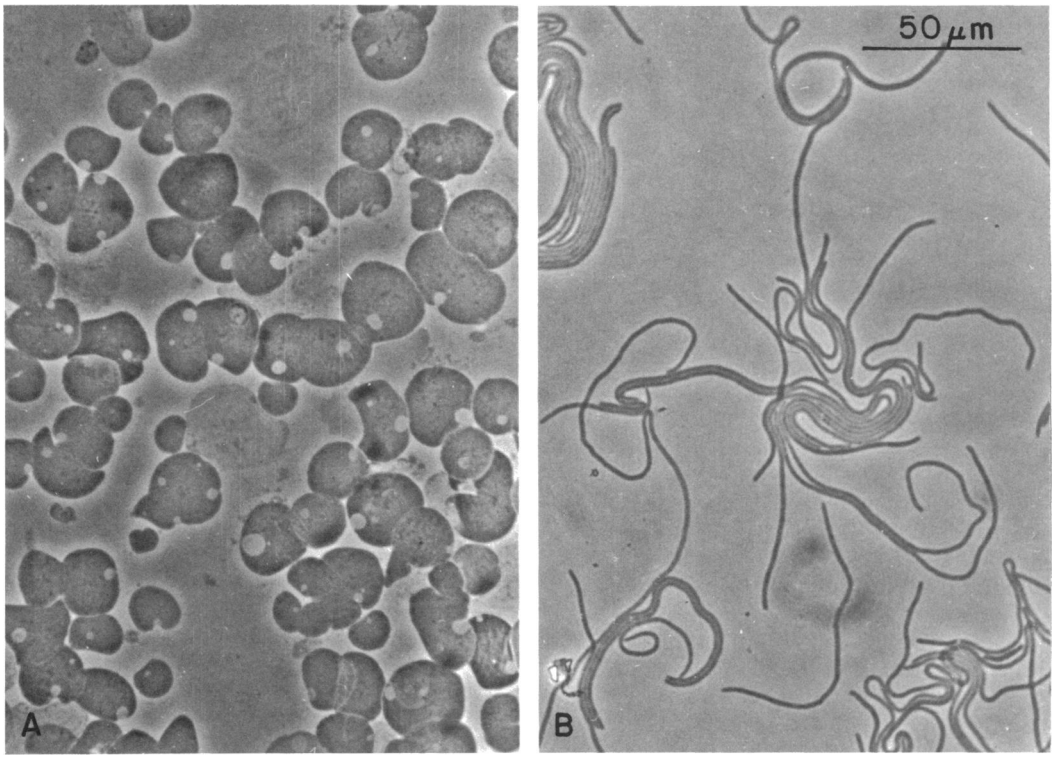

FIG. 4. *Phase photomicrograph of BU8049 grown in NaLB, 3 h after irradiation on agar slip. (A) Preincubation of cells in 1 μg of FL1060 per ml before irradiation. (B) No exposure to FL1060.*

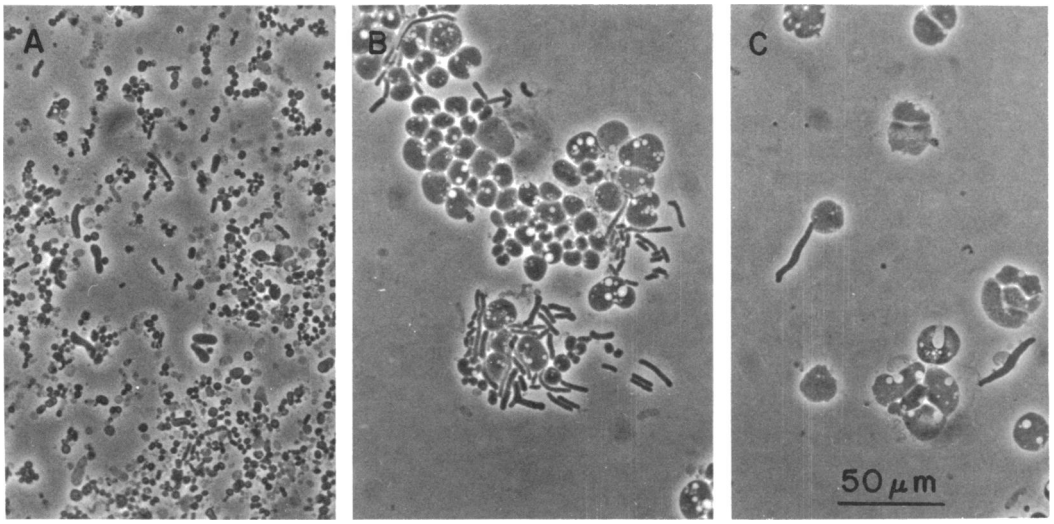

FIG. 5. *Phase photomicrograph of LL9 grown in NaLB, 3 h after plating. (A) Cells grown in 0.1 μg of FL1060 per ml, no irradiation. (B) Cells grown in 0.3 μg of FL1060 per ml, no irradiation. (C) Cells grown in 0.3 μg of FL1060 per ml + irradiation at time of plating. Compare with Fig. 2 and 6 for cells irradiated without exposure to FL1060.*

the density of cells in Fig. 5B is greater than that in C. Crowding in irradiated cultures of giant-cell-producing strains appears to retard formation of the largest cells (possibly by promoting cell division), so that it seems unwarranted to conclude that the giant cells from FL1060-treated cultures are larger if irradiated.

The culture of LL9 in Fig. 6 received irradiation without exposure to FL1060. The filaments (B) are longer than any in Fig. 5, and the giant cells are more irregular; both effects may be traced to the scarcity of rounded forms in log-phase cultures not exposed to the drug.

The length of pretreatment in FL1060 seemed to have no effect on giant-cell size in irradiated cultures. Cells incubated for 90 min before irradiation and cells exposed to the drug at the time of irradiation produced the same range of maximal size. This finding suggests that there exists a maximal size for plated cells, beyond which lysis occurs. The same conclusion was reached from time-lapse studies on plated, irradiated cells of LL9.

The dosage for induction of the morphological change in this study depends on the presence of *envB* or *mon*. Strains LL11 (*mon-1*) and LL9 (*envB1*) became rounded at 0.3 μg of FL1060 per ml, whereas the *envB*$^+$ strains BU8049, W3110, and LL6 (from which LL9 and LL11 were derived) required 1 μg/ml before morphological change occurred. The state of the *lon* allele had no effect on the dosage levels in any strains tested.

For simple production of giant cells, incubation with FL1060 is the method of choice. With the estimate that cells of strains tested are 1.5 to 2 μm thick when grown on agar plates, the largest FL1060-induced cells reach 500 to 700 μm^3, comparable to the largest cells produced by the double mutants described above. The generality of the response to FL1060 means that giant cells can be obtained in a wide variety of strains without the genetic alterations.

Stability and viability. As had been observed for P678-A4, all genetically constructed giant-cell-producing strains reverted to predominantly rods or irregular cells much reduced in volume after repeated subculturing or after storage at low temperature. After the transition, irradiation failed to produce giant cells; rod-filled suspensions gave rise predominantly to filaments, while the small heteromorphic popula-

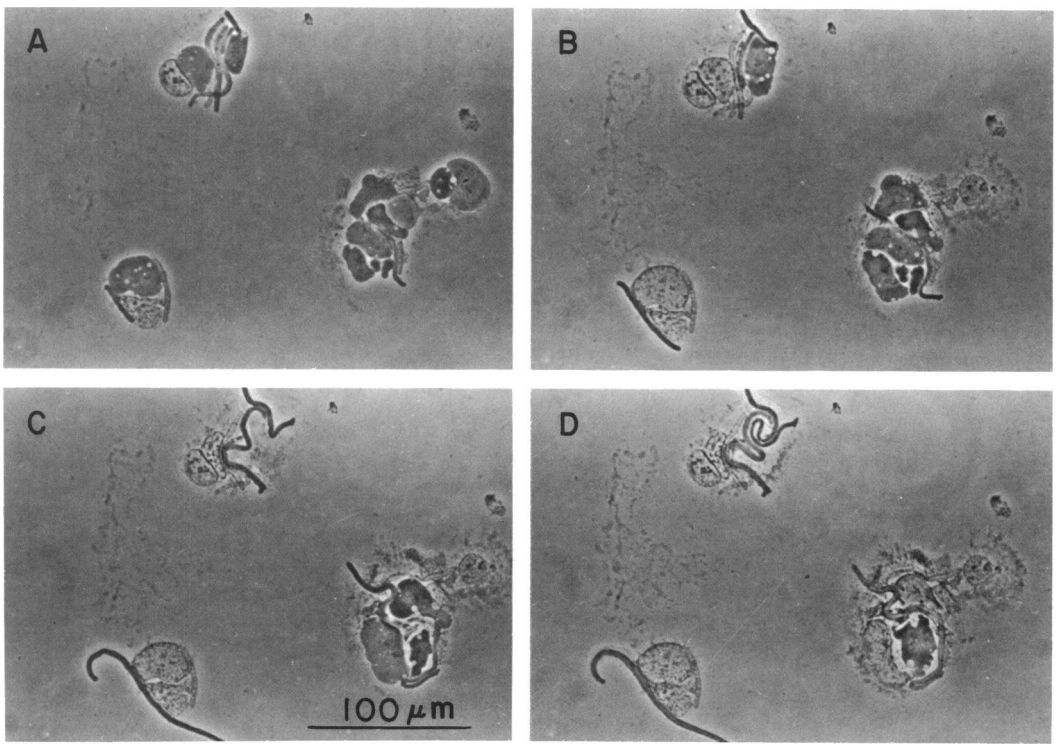

FIG. 6. *Phase photomicrograph of growth of LL9 giant cells on NaGCB agar slip. Time elapsed since irradiation: (A) 50 min; (B) 99 min; (C) 154 min; (D) 205 min.*

tions produced mostly bizarre forms and irregular filaments under the same conditions. Strain LL8, for example, reverted to rods within a month after its construction. Raised from a purified isolate of the original Amp^s transductant, the strain became Amp^r simultaneously with its reversion to rods. This finding suggests that an Amp^r revertant overgrew the Amp^s cells of the original transductant. On the other hand, LL81 also reverted to a collection of small irregular cells but maintained its ampicillin sensitivity.

Storage in the cold is more rapidly lethal to giant-cell-producing strains than to many other mutants in the collection of this laboratory. This applies to storage on plates at 4°C or storage in glycerolized cultures at −20°C. Lyophilization has proved the most effective means of storing the strains. Differential viability (in the cold) among the morphological variants in any given strain may contribute to the instability described, but in the absence of knowledge of the genetic basis for the phenotypic variability, many other explanations are also possible.

Growth of giant cells on agar after UV irradiation. In a single experiment, the growth of nine cells of LL9 on thin NaGCB plates was photographed at 50, 67, 83, 99, 117, 137, 154, 175, 190, and 205 min after irradiation (150 ergs/mm^2). The cells and supporting agar were mounted between slide and cover slip shortly before the first photograph (i.e., after 45 min of incubation at 37°C). The slide was returned to the incubator in a moist chamber between shots. Comparison of the unmounted culture with that photographed showed no difference in condition of the population at the end of the experiment. Figure 6 presents the cultures at 50 (top right), 99 (top left), 154 (bottom right), and 205 min.

The obvious heterogeneity, including filaments and bizarres, is typical of giant-cell-producing strains. All cells grew during the experiment, and all lysed during the period of observation except one bizarre, which grew into a giant cell. Vacuolation in irregular cells became more prominent as cell size increased; even filamentous forms typically showed vacuoles, though not in the examples of Fig. 6.

Surface area was measured with a compensating polar planimeter and gave errors (in triplicate estimates) ranging from 10% for the smallest cells to less than 5% for large cells. Since phase microscopy blurred the cell edge because the cells were not perfectly flat, and since the cells shifted relative to one another during growth, the error seems acceptable. The individual growth curves (surface area [S] versus time) were smooth and allowed extrapolation to S_0 (surface area at time of irradiation). The growth curves of giant cells and bizarres permitted linear approximation and easy calculation of doubling times; those of filaments were roughly hyperbolic, with a definite slowing in growth rate toward the end of the experiment.

The doubling times of individual cells ranged from 35 to 45 min for the filaments and smallest bizarres (S_{50} = 15 μm^2) to 95 to 145 min for the larger cells (S_{50} = 100 μm^2). We determined an average doubling time of 60 to 70 min by plotting a normalized value of increasing surface area (S_t/S_{50}) against time; the value is almost twice the doubling time of 35 to 40 min routinely measured in shaking cultures of LL9 (in NaGCB, 37°C) before irradiation.

Cells lysed at different times throughout the experiment, and survival correlated (inversely) with surface area rather than with time after irradiation. Most giant cells disintegrated at an area of 150 to 250 μm^2, and only the filaments and one giant cell survived for more than 3 h after irradiation.

Figure 7 shows the correlation of doubling times and survival times with S_0. The smallest cells, regardless of morphology, grew the most rapidly and survived the longest. The result is not unexpected because growth and division are known to be closely related to the maintenance of normal morphology. The loss of division in the presence of a constant surface/volume ratio, as in filaments, leads to slowed growth and cell death, as illustrated in this experiment.

The increase in surface area (or volume) during the period of observation ranged from 1.8 for the largest cells to 30 for the smallest, if S_0

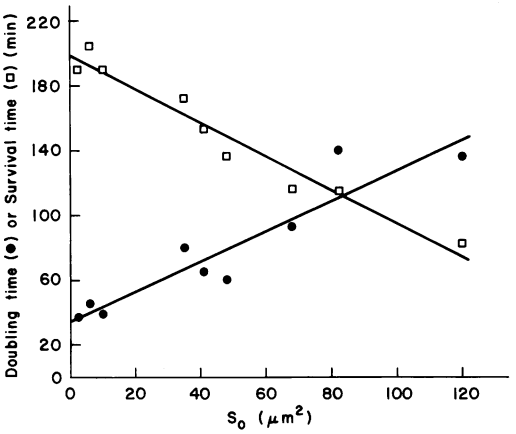

FIG. 7. *Correlation of doubling times and survival times, after irradiation, with S_0 (the surface areas) of nine cells of LL9 (Fig. 6) at time of plating and irradiation. (The lines are drawn by eye.)*

is used for the comparison. The range is 1.5 to 12, with S_{50} as the index.

The giant cells were shaped like pancakes when grown on an agar surface, and, when washed from plates with NaGCB, they were measured to be 1.5 to 2 μm thick. The cells in this study, therefore, reached 300 to 500 μm^3 at time of lysis.

DISCUSSION

Comparison of genetic and pharmacological giant-cell types. The approaches we have used in these experiments have been successful in producing giant cells of *E. coli* K-12 that have a rather limited life-time but which are nevertheless proving useful in evaluating microelectrode techniques with this organism (H. Felle and C. L. Slaymen, unpublished data). Both varieties of the giant cells take advantage of conditions that inhibit cell division and confer a rounded-cell shape. The genetic approach is similar to that of Adler et al. (1). Inhibition of cell division was achieved by introducing any one of several *lon* (= *capR* = *degTa*) mutations, which result in inhibition of septum formation after UV irradiation. Although the nature of the *lon* gene product is not yet understood, it seems to be involved in the degradation of defective proteins (20, 21).

The *envB* mutation, which we have used to introduce the rounded morphology, leads to a cell population that is very heterogeneous in size, shape, and plane of division (5). As expected, the Lon^- and $EnvB^-$ phenotypes were additive so that, after UV irradiation, septation stopped (as in Lon^-) and cell shape remained amorphous and heterogeneous (as in $EnvB^-$). This result is consistent with Adler's observation for the *lon mon* strain, since we have found *mon* to be probably allelic with *envB*.

The morphological phenotype induced by the drug FL1060 was similar to that caused by *envB*, but the drug also blocked septation, as had been reported by James et al. (8). (Much earlier, aberrant morphology had been noted after penicillin treatment. Many of the forms reported by those workers were similar to ours, but generally the cell size was smaller [19].) Thus, we observed giant-cell production by FL1060 whether the strain carried *lon* or lon^+. It is interesting that many of the FL1060-resistant mutants isolated by Matsuhashi et al. (15) are spherical in shape and might be *envB*, suggesting a similar target in the cell for FL1060 and the *envB* gene product. James et al. (8) reported that there is no direct effect of FL1060 on DNA, RNA, or protein synthesis, but we have not tested giant cells in later stages of growth to see how long this state is maintained.

It is tempting to speculate that the greater morphological homogeneity in FL1060-treated cultures (Fig. 4A) results from uniform binding of the drug to all sensitive sites, whereas in *envB* strains a partially effective protein is active in formation of the cell surface.

In many other ways, the giant cells obtained pharmacologically were comparable to those obtained genetically. (i) Maximal volumes of both were about 500 μm^3, 200 to 500 times the volume of wild-type *E. coli*. (ii) Vacuolation was present in both types of giant cells, though the vacuoles were generally larger and sparser in FL1060-treated cells. (iii) Lifetime: soon after reaching maximal volume, cells of both types disintegrated, so that, given the different means of production and the various genetic makeup of the strains, the disruption seems due to common physical constraints.

Both approaches to giant-cell production were sensitive to growth media. Use of supplemented minimal media, instead of the rich media, gave smaller cells in all cases. With the *lon envB* strains, for example, NaGCB yielded log-phase cells twice the volume of those raised in NaLB and LB, and this difference was maintained in the giant cells of the irradiated cultures. LB medium tended to reduce the production of giant cells and bizarre forms in favor of filaments. The giant cells washed from NaGCB plates with liquid NaGCB were rigid pancakes with irregular edges; when isosmolar sucrose solutions were added to the cell suspensions, the cells (LL81 in a test case) lost their rigidity and rounded up, suggesting that electrostatic interactions are important to maintenance of rigid shape in the giant cells. Recent experiments with FL1060 giants (H. Felle and C. L. Slayman, unpublished data) have indicated that lowered growth temperature (23 to 25°C, instead of the usual 37°C) reduces the dependence of size and morphology on composition of the medium. Cell volumes of 100 to 1,000 μm^3 are obtained on giant-cell broth with the added sodium largely substituted by sucrose, and both size and shape are retained upon transfer of these cells to isotonic sucrose or even to dilute media.

Growth curves of agar-cultured cells were measured only for genetic giants, mostly from LL81. Pre-irradiation log-phase cells of that strain were found to be 10- to 20-fold the volume of normal rods, and to have volume-doubling times (averaged over the whole population) of 45 min. Six hours after UV irradiation, average volumes had increased 12-fold, so that volume doubling had occurred three to four times during that interval, for an average doubling time of

100 min. Growth rates ($\Delta S/\Delta t$) among different cell shapes varied widely, but were generally sigmoid, with lags after irradiation and before final disruption. The differing growth rates correlated with size (inversely) and morphology of the log-phase cells at the time of irradiation. As shown in Fig. 5, the smaller cells of LL9 (rods and small bizarres destined to become filaments and giant cells, respectively) doubled more rapidly than the larger bizarre forms. Bloom et al. (5) have reported a similar phenomenon among the log-phase cells of D23 grown on agar; the smaller, more regular cells of the heteromorphic cultures divide more rapidly than do the larger, more bizarre forms.

The observed difference in growth rates among morphological types allows one to explain the instability of the giant-cell strains as the overgrowth of the original heteromorphic population by faster-growing rods. The same explanation accounts for the rather inconstant log-phase doubling times with filament-producing cultures.

Genetics aspects of giant-cell phenotype. The correlation of morphology with various combinations of *sloB, rpsL, envB,* and *rpsE* allowed us to determine that only *envB* is directly responsible for the irregular shape in our transductant series. A similar conclusion was published by Westling-Häggström and Normark during the course of these experiments (23). The other mutant loci in these transductant series interact in various ways with *envB*. The following discussion will examine the interaction in terms, first, of modification of EnvB$^-$ morphology and, second, of the dissociation of morphology and ampicillin resistance.

I. *Modification of abnormal morphology.*

(A) The *rpsL* genotype seems to affect the severity of expression of the EnvB$^-$ morphology. In Tables 2 and 4, class VI (*rpsL*) transductants show less bizarre forms and a less heteromorphic culture than those in class VIII (*rpsL*$^+$). The *rpsL* allele is known to restrict certain cases of genetic suppression (22), and such a mechanism is at least hypothetically possible in the present case.

(B) *rpsE* has been found to relieve the restriction imposed by *rpsL* in a nonsense suppression system (22). *rpsE rpsL* transductant strains show greater morphological irregularity than corresponding *rpsE*$^+$ *rpsL* strains, e.g., classes VI, R and S, and VIII, R and S, in Table 4.

(C) The effect of *sloB* on the morphology of *envB* mutants is difficult to assess because of the close linkage between *sloB* and *rpsL* loci in donor strains, as shown by the low frequencies of classes III to VI in Table 2. Nonetheless, the effect of *sloB* on production of abnormal morphology appears minor, since irregular cells occur in both Slo$^-$ and Slo$^+$ backgrounds.

II. *Dissociation of Amp^s and Morph$^-$ phenotypes.*

Three more transductions are relevant to the discussion of dissociation of phenotypes. (i) P1 · LL81 × LL57 and (ii) P1 · D23 × 1157 with Str^r selection both showed greater cotransduction frequency for *rpsL*-Amp^s (85%) than for *rpsL-aroE*$^+$ (34%). Eight Amp^s transductants checked for morphology were all rods, or chains of rods and filaments. (iii) Westling-Häggström and Normark (22) performed the transduction P1 · G11 (*ilv metB ampA*$^+$) × D23 and selected fast-growing Amp^r transductants. They report a cotransduction frequency for Amp^r-*rpsL*$^+$ of 42%, a very high figure for two markers so far apart on the genome.

The three transductions share two characteristics. First, there was an unexpectedly low frequency of transduction, $N = 74$ in our two transductions and 32 in the work of the Swedish investigators. This suggests the production of many inviable transductants. Second, in both sets of transductions the highest frequencies observed were in the double-crossover class and in the class with the longest stretch of donor genome transferred (if one assumes that Amp^s and Amp^r identify *envB* and *envB*$^+$, respectively). Their largest classes were *rpsL*$^+$-Amp^r whereas ours were *rpsL*-Amp^s. They concluded that "D23 contained a second mutation close to *strA* which affected the phenotype of the mutant strain," i.e., *sloB*.

(A) *sloB* cannot be the sole cause for the dissociation, which has been found in both Slo$^-$ and Slo$^+$ transductants (involving the closely related *envB* and *mon* sites). The simultaneous disappearance of the Slo$^-$ phenotype and of the dissociation in the transductant series of Table 3, however, suggests that *sloB* may be involved with other loci in creating the dissociation. Very little is known of the biochemical basis for the slow growth attributed to *sloB;* its close linkage to *rpsL* suggests that it may be involved in production of ribosomal proteins, like many other loci in that region of the genome. Pleiotropic effects and interactions of mutations in that region have been described (21).

(B) *rpsL* seems a more likely candidate for involvement in the dissociation of ampicillin resistance and the morphological effects of *envB*. In our transductant series, all classes showing the dissociation are *rpsL*: *sloB rpsL* in Table 2, *sloB*$^+$ *rpsL* in Table 4, and *sloB rpsL* in the Str^r series reported above. Possibly dissociation is the result of an *rpsL*-directed restriction of

suppression, and the introduction of the *rpsE* mutation could lead to the loss of dissociation as shown in Table 3.

(C) All the transductants reported in this paper are present in an *ampA* background. If this mutation is suppressible, we might explain the unexpected ampicillin sensitivity of class I transductants as the result of decreased penicillinase production when *rpsL* is present to restrict the suppression of *ampA,* thus accounting for the dissociation of ampicillin sensitivity and morphology.

ACKNOWLEDGMENTS

We thank H. I. Adler, Oak Ridge National Laboratory, for encouraging the initial work; Leo Pharmaceutical Products, Ltd., Ballerup, Denmark, for a generous supply of FL1060; and Tom McLaughlin for expert technical assistance throughout the experiments.

The research was supported by Public Health Service program project grant AM-17433 from the National Institute of Arthritis, Metabolism and Digestive Diseases, and by Public Health Service grant CA-06519 from the National Cancer Institute.

LITERATURE CITED

1. **Adler, H. I., C. E. Terry, and A. A. Hardigree.** 1968. Giant cells of *Escherichia coli.* J. Bacteriol. **95**:139–142.
2. **Allison, D. P.** 1971. Giant cells of *Escherichia coli*: a morphological study. J. Bacteriol. **108**:1390–1401.
3. **Anderson, P., Jr.** 1969. Sensitivity and resistance to spectinomycin in *Escherichia coli.* J. Bacteriol. **100**:939–947.
4. **Bachmann, B. J., K. B. Low, and A. L. Taylor.** 1976. Recalibrated linkage map of *Escherichia coli* K-12. Bacteriol. Rev. **40**:116–167.
5. **Bloom, G. D., J. Gumpert, S. Normark, E. Schumann, U. Taubeeck, and B. Westling.** 1974. Morphology and growth pattern of a rod-negative *envB* mutant of *Escherichia coli* K-12. Z. Allg. Mikrobiol. **14**:465–477.
6. **Bukhari, A. I., and D. Zipser.** 1973. Mutants of *Escherichia coli* with a defect in the degradation of nonsense fragments. Nature (London) New Biol. **243**:238–241.
7. **Castellazzi, M., J. George, and G. Buttin.** 1972. Prophage induction and cell division in *E. coli.* I. Further characterization of a thermosensitive mutation *tif-1* whose expression mimics the effect of UV-irradiation. Mol. Gen. Genet. **119**:139–152.
8. **James, R., J. Y. Haga, and A. B. Pardee.** 1975. Inhibition of an early event in the cell division cycle of *Escherichia coli* by FL1060, an amidinopenicillanic acid. J. Bacteriol. **122**:1283–1292.
9. **Kirby, E. P., F. Jacob, and D. A. Goldthwait.** 1967. Prophage induction and filament formation in a mutant strain of *Escherichia coli.* Proc. Natl. Acad. Sci. U.S.A. **58**:1903–1910.
10. **Kohiyama, M. D., D. Cousin, A. Ryter, and F. Jacob.** 1966. Mutants thermosensibles d'*Escherichia coli* K-12. Ann. Inst. Pasteur **110**:465–486.
11. **Lloyd, R. G., B. Low, G. N. Godson, and E. A. Birge.** 1974. Isolation and characterization of an *Escherichia coli* K-12 mutant with a temperature-sensitive RecA$^-$ phenotype. J. Bacteriol. **120**:407–415.
12. **Low, B.** 1973. Rapid mapping of conditional and auxotrophic mutations in *Escherichia coli* K-12. J. Bacteriol. **113**:798–812.
13. **Low, B., F. Gates, T. Goldstein and D. Söll.** 1971. Isolation and partial characterization of temperature-sensitive *Escherichia coli* mutants with altered leucyl- and seryl-transfer ribonucleic acid synthetases. J. Bacteriol. **108**:742–750.
14. **Markovitz, A.** 1964. Regulatory mechanisms for synthesis of capsular polysaccharide in mucoid mutants of *Escherichia coli* K-12. Proc. Natl. Acad. Sci. U.S.A. **51**:239–246.
15. **Matsuhashi, S., T. Kamiryo, P. M. Blumberg, P. Linnett, E. Willoughby, and J. L. Strominger.** 1974. Mechanism of action and development of resistance to a new amidino penicillin. J. Bacteriol. **117**:578–587.
16. **Melchior, N. H., J. Blom, L. Tybring, and A. Birch-Andersen.** 1973. Light and electron microscopy of the early response of Escherichia coli to a 6β-amidinopenicillanic acid (FL1060). Acta Pathol. Microbiol. Scand. Sect. B **81**:393–407.
17. **Mitchell, P.** 1961. Coupling of phosphorylation to electron and hydrogen transfer by a chemiosmotic type of mechanism. Nature (London) **191**:144–148.
18. **Normark, S.** 1969. Mutation in *Escherichia coli* K-12 mediating spherelike envelopes and changed tolerance to ultraviolet irradiation and some antibiotics. J. Bacteriol. **98**:1274–1277.
19. **Shanahan, A. J., A. Eisenstark, and F. W. Tanner.** 1947. Morphology of Escherichia coli exposed to penicillin as observed with the electron microscope. J. Bacteriol. **54**:183–189.
20. **Shineberg, B., and D. Zipser.** 1973. The *lon* gene and degradation of β-galactosidase nonsense fragments. J. Bacteriol. **116**:1469–1471.
21. **Slater, M., and M. Schaechter.** 1974. Control of cell division in bacteria. Bacteriol. Rev. **38**:199–221.
22. **Weisblum, B., and J. Davies.** 1968. Antibiotic inhibitors of the bacterial ribosome. Bacteriol. Rev. **32**:493–528.
23. **Westling-Häggström, B., and S. Normark.** 1975. Genetic and physiological analysis of an *envB* spherelike mutant of *Escherichia coli* and characterization of its transductants. J. Bacteriol. **123**:75–82.